ELECTRONIC SUPPORTING INFORMATION

Deep eutectic solvent promoted one step sustainable conversion of fresh seaweed biomass to functionalized graphene as potential electrocatalyst

Dibyendu Mondal, [a,d] Mukesh Sharma,[a,d] Chen-Hao Wang,[e] Yu-Chuan Lin,[e] Hsin-Chih Huang,[e] Arka Saha,[c,d] Sanna Kotrappanavar Nataraj [b,d]* and Kamalesh Prasad [a,d]*

[a] *Marine Biotechnology and Ecology Division, CSIR-Central Salt & Marine Chemicals Research Institute, G. B Marg, Bhavnagar 364002 (Gujarat), India* [Corresponding author : e-mail : *kamlesh@csmcri.org/drkamaleshp@gmail.com]; Phone No.: +91-278 2567760. Fax No. +91-278-2567562*

[b] *Centre for Nano and Material Science, Jain University, Bangalore-562112 [sknata@gmail.com; sk.nataraj@jainuniversiy.co.in]*

[c] *Inorganic Materials & Catalysis Division, CSIR-Central Salt & Marine Chemicals Research Institute, G. B Marg, Bhavnagar 364002 (Gujarat), India*

[d] *Academy of Scientific and Innovative Research (AcSIR), Central Salt & Marine Chemicals Research Institute, G. B Marg, Bhavnagar 364002 (Gujarat), India*

[e] *Department of Materials Science and Engineering, National Taiwan University of Science and Technology, 106 Taipei, Taiwan.*

Table S1: Composition of the sap extracted from *Sargassum tenerrimum*.

Element/Growth regulators	Na	K	Ca	Mg	Zn	Cu	Mn	Indole 3-acetic acid	Zeatin	GA_9*
	ppm									
Sargassum sap	574	318	123	122	2.3	0.6	0.8	13.2	11.4	detected

* K. Prasad, A.K. Das, M.D. Oza, H. Brahmbhatt, A.K. Siddhanta, R. Meena, K. Eswaran, M.R. Rajyaguru, P.K. Ghosh. Detection and quantification of some plant growth regulators in a seaweed-based foliar spray employing a mass spectrometric technique sans chromatographic separation. *J Agr. Food Chem*., 2010, **58**, 4594-4601.

Table S2: Elemental composition of granule obtained after removing the sap from *Sargassum tenerrimum*

.

Elements	Na	K	Ca	Mg	Fe	Zn	Cu	Mn	C	H	N	S
	% wt											
Sargassum granules	1.18	0.73	1.99	1.16	0.0	0.014	0.00022	0.0017	34.1	4.88	1.43	0.80

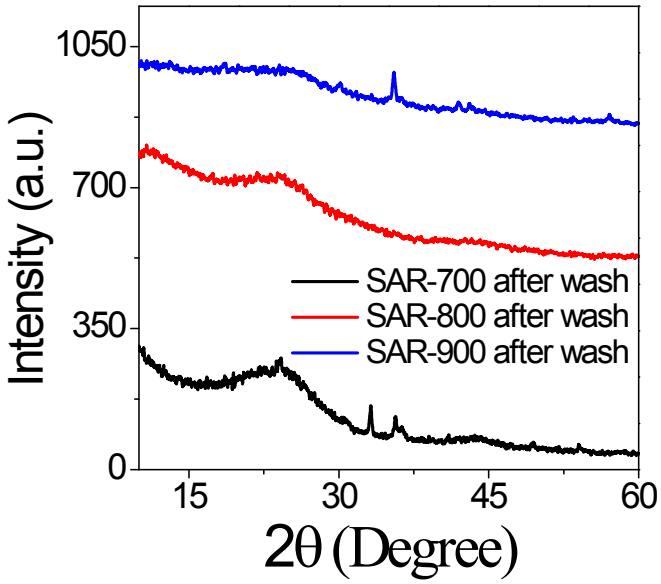

Figure S1: Powder XRD patterns of graphene nanosheets recorded after washing with 6N HCl solution to remove iron.

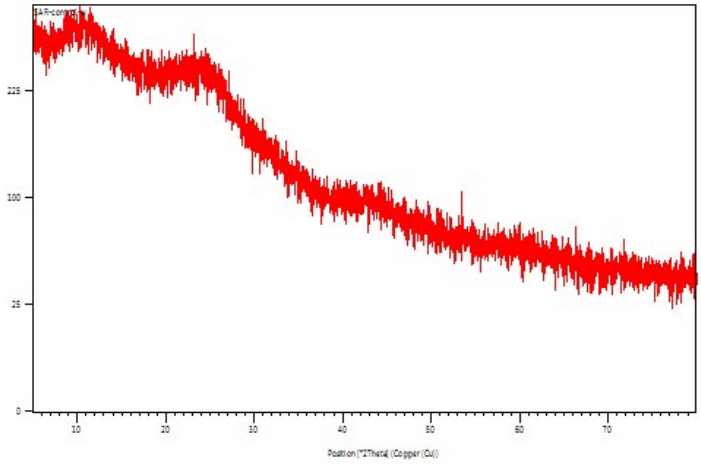

Figure S2 : Powder XRD patterns of carbon obtained at pyrolysis at 700 oC for *Sargassum tenerrimum* seaweed without doping.

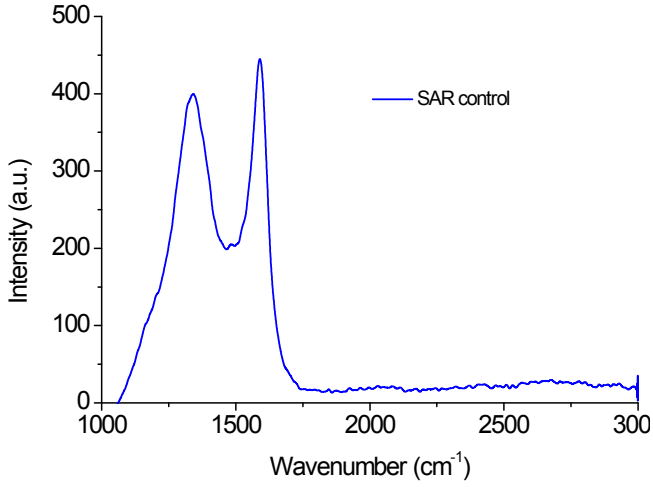

Figure S3 : Raman spectra of carbon obtained at pyrolysis at 700 oC for *Sargassum tenerrimum* seaweed without doping.

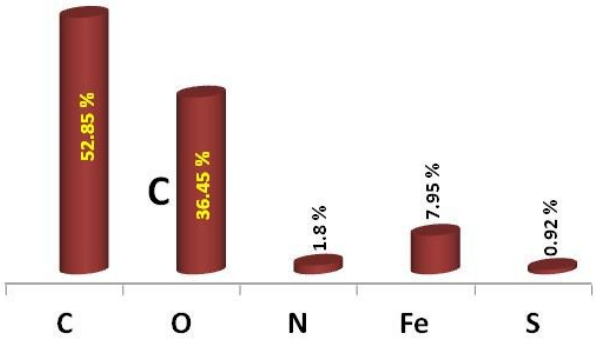

Figure S4 : Atom% of SAR-700 measured using XPS.

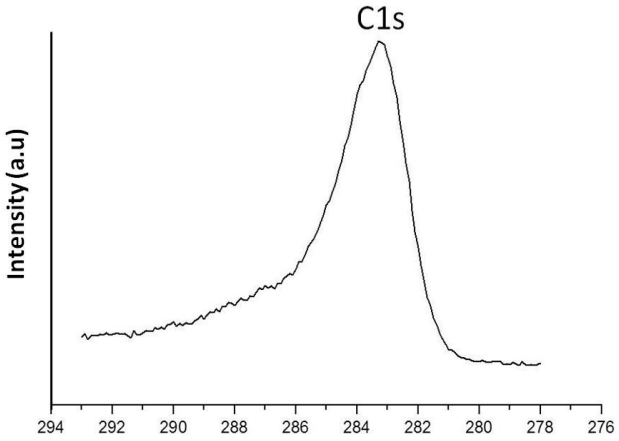

Figure S5 : High resolution C1s XPS spectra of SAR-700

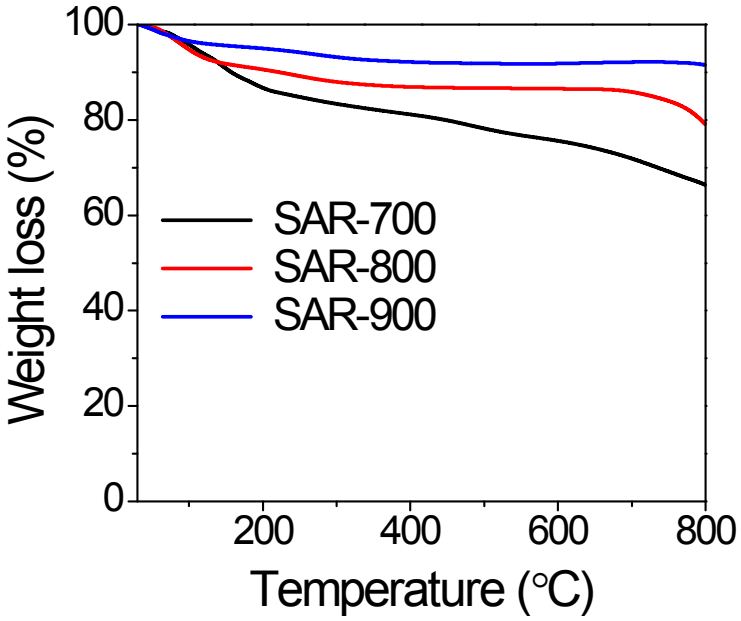

Figure S6: TGA plot for Fe_3O_4/Fe doped graphene nanosheets obtained after calcined the SAR-ChoCl-$FeCl_3$ composited at 700 ºC (SAR-700), 800 ºC (SAR-800) and 900 ºC (SAR-900) , respectively.

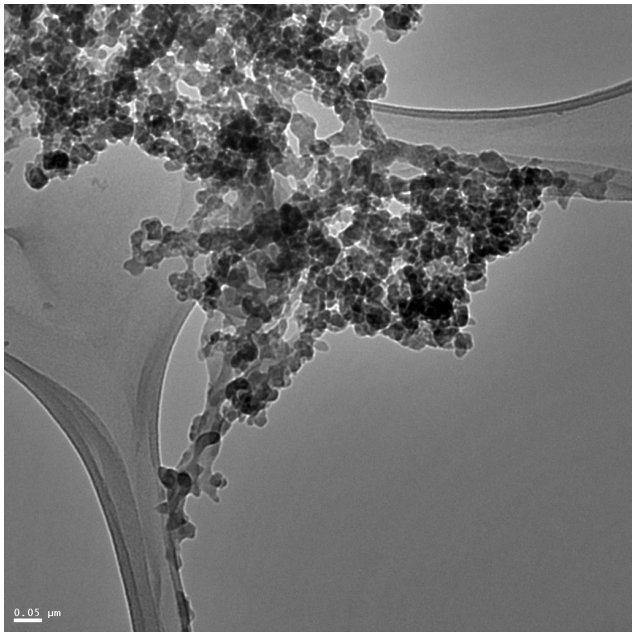

Figure S7 : TEM image of carbon obtained at pyrolysis at 700 oC for *Sargassum tenerrimum* seaweed without doping.

Table S3: Comparison of the specific surface area of this work to literature reports

Entry	Materials	S_{BET} ($m^2.g^{-1}$)	Reference
1	Carbon/Graphene aerogel	254	1
2	Polypyrrole-mediated Graphene Foam	151	2
3	CNT/RGO architecture	224	3
4	3D macroporous graphene frameworks	194	4
5	3D N-doped graphene aerogel supported Fe_3O_4 nanoparticles	110	5
6	Nanoporous Fe_3O_4–carbon nanosheets	229	6
7	Magnetite-graphene hybrids	148	7
8	3D hierarchical Fe_3O_4–graphene nanosheets	52.84	8
9	Hollow-Fe_3O_4 graphene hybrid sheet	45.9	9
10	Graphitic N-doped carbon-supported Fe3O4 nanoparticles	210.6	10
11	SAR-700	220	Present study
12	SAR-800	168	
13	SAR-900	132	

Reference:

1. Liu, R.; Wan, L.; Liu, S.; Pan, L.; Wu, D.; Zhao, D. An Interface-Induced Co-Assembly Approach Towards Ordered Mesoporous Carbon/Graphene Aerogel for High-Performance Supercapacitors. *Adv. Funct. Mater.,* **2015**, *25*, 526–533.
2. Zhao, Y.; Liu, J.; Hu, Y.; Cheng, H.; Hu, C.; Jiang, C.; Jiang, L.; Cao, A.; Qu, L. Highly Compression-Tolerant Supercapacitor Based on Polypyrrole-mediated Graphene Foam Electrodes. *Adv. Mater.*, **2013**, *25*, 591–595.
3. Jha, N.; Ramesh, P.; Bekyarova, E.; Itkis, M. E.; Haddon, R. C. High Energy Density Supercapacitor Based on a Hybrid Carbon Nanotube-Reduced Graphite Oxide Architecture. *Adv. Energy Mater.*, **2012**, *2*, 438–444.
4. Choi, B. G.; Yang, M.; Hong, W. H.; Choi, J. W.; Huh, Y. S. 3D Macroporous Graphene Frameworks for Supercapacitors with High Energy and Power Densities. *ACS Nano*, **2012**, *6*, 4020–4028.
5. Wu, Z.-S.; Yang, S.; Parvez, K.; Feng, X.; Müllen, K. 3D Nitrogen-Doped GrapheneAerogel-Supported Fe3O4 Nanoparticles as Efficient Electrocatalysts for the Oxygen Reduction. *J. Am. Chem. Soc.*, **2012**, *134*, 9082–9085.
6. Liu, D.; Wang, X.; Wang, X.; Tian, W.; Liu, J.; Zhi, C.; He, D.; Bandoa, Y.; Golberg, D. Ultrathin nanoporous Fe3O4–carbon nanosheets with enhanced supercapacitor performance. *J. Mater. Chem. A*, **2013**, *1*, 1952–1955.
7. Chandra, V.; Park, J.; Lee, J. W.; Hwang, I.-C.; Kim, K. S. Water-Dispersible Magnetite-Reduced Graphene Oxide Composites for Arsenic Removal. *ACS Nano*, **2010**, *4*, 3979–3986.
8. Li, X.; Huang, X.; Liu, D.; Wang, X.; Song, S.; Zhou, L.; Zhang, H. Synthesis of 3D Hierarchical Fe3O4/Graphene Composites with High Lithium Storage Capacity and for Controlled Drug Delivery. *J. Phys. Chem. C*, **2011**, *115*, 21567–21573.
9. Wang, R.; Xu, C.; Sun, J.; Gao, L.; Lin, C. Flexible free-standing hollow Fe_3O_4/graphene hybrid films for lithium-ion batteries. *J. Mater. Chem. A*, **2013**, *1*, 1794–1800.
10. Su, Y.; Jiang, H.; Zhu, Y.; Yang, X.; Shen, J.; Zou, W.; Chen, j.; Li, C. Enriched graphitic N-doped carbon-supported Fe_3O_4 nanoparticles as efficient electrocatalysts for oxygen reduction reaction. *J. Mater. Chem. A*, **2014**, *2*, 7281–7287.